OXFORD

Cerebral Cortex, 2023, **33**, 10546–10557
https://doi.org/10.1093/cercor/bhad302
Advance access publication date 16 August 2023
Original Article

Shank3 mutations enhance early neural responses to deviant tones in dogs

Liang Wu[1,2,†], Shuting Mei[3,†], Shan Yu[4], Shihui Han[3,*], Yong Q. Zhang[1,2,*]

[1]State Key Laboratory for Molecular and Developmental Biology, Institute of Genetics and Developmental Biology, Chinese Academy of Sciences, Beijing 100101, China,
[2]College of Life Sciences, University of Chinese Academy of Sciences, Beijing 100049, China,
[3]School of Psychological and Cognitive Sciences, PKU-IDG/McGovern Institute for Brain Research, Beijing Key Laboratory of Behavior and Mental Health, Peking University, Beijing 100871, China,
[4]Brainnetome Center and State Key Laboratory of Pattern Recognition, Institute of Automation, Chinese Academy of Sciences, Beijing 100190, China
*Corresponding authors: Shihui Han, School of Psychological and Cognitive Sciences, PKU-IDG/McGovern Institute for Brain Research, Beijing Key Laboratory of Behavior and Mental Health, Peking University, Beijing 100871, China. Email: shan@pku.edu.cn; Yong Q. Zhang, State Key Laboratory for Molecular and Developmental Biology, Institute of Genetics and Developmental Biology, Chinese Academy of Sciences, Beijing 100101, China. Email: yqzhang@genetics.ac.cn
†Liang Wu and Shuting Mei contribute equally to this work.

Both enhanced discrimination of low-level features of auditory stimuli and mutations of *SHANK3* (a gene that encodes a synaptic scaffolding protein) have been identified in autism spectrum disorder patients. However, experimental evidence regarding whether *SHANK3* mutations lead to enhanced neural processing of low-level features of auditory stimuli is lacking. The present study investigated this possibility by examining effects of *Shank3* mutations on early neural processing of pitch (tone frequency) in dogs. We recorded electrocorticograms from wild-type and *Shank3* mutant dogs using an oddball paradigm in which deviant tones of different frequencies or probabilities were presented along with other tones in a repetitive stream (standards). We found that, relative to wild-type dogs, *Shank3* mutant dogs exhibited larger amplitudes of early neural responses to deviant tones and greater sensitivity to variations of deviant frequencies within 100 ms after tone onsets. In addition, the enhanced early neural responses to deviant tones in *Shank3* mutant dogs were observed independently of the probability of deviant tones. Our findings highlight an essential functional role of *Shank3* in modulations of early neural detection of novel sounds and offer new insights into the genetic basis of the atypical auditory information processing in autism patients.

Key words: auditory processing; autism; dog; electrocorticogram; Shank3.

Introduction

Autism spectrum disorder (ASD) is a lifelong neurodevelopmental disorder observed in large populations (Lord et al. 2020). Besides showing social communicative impairment and repetitive behaviors, autistic individuals exhibit atypical sensory reactions to stimuli, which has been considered as a core feature of the condition (American Psychiatric Association 2013). Auditory hypersensitivity including superior pitch discrimination (Ferri et al. 2003; Bonnel et al. 2010) and enhanced auditory evoked responses (Lepistö et al. 2005; Wang et al. 2006; Roberts et al. 2011) is particularly common in ASD (Williams et al. 2021). In addition, auditory dysfunction is severe in ASD paitents with language impairments (Roberts et al. 2011) and could be used to predict autistic traits (Brandwein et al. 2015). Given the accumulating evidence indicating an etiologic role of genetic defects in ASD (Chen et al. 2015; Tremblay and Jiang 2019), one may expect that genetic mutations also contribute to the hypersensitivity of auditory processing observed in autism. However, to date, there has been little experimental evidence for a causal role of a specific genetic mutation in the atypical auditory processing. The present study sought to address this issue by testing a possible association between *Shank3* mutation and the ASD-like atypical auditory processing in an animal model.

SHANK3 is a scaffolding protein localized at excitatory synapses (Naisbitt et al. 1999). Patients carrying mutations in *SHANK* gene family including *SHANK3*, which accounts for ~ 1% of idiopathic forms of ASD (De Rubeis et al. 2018), often exhibit global developmental delay and autistic behavior (Phelan and McDermid 2012). Previous studies have revealed social impairments and stereotypical behaviors in *SHANK3* mutant macaques (Zhao et al. 2017; Tu et al. 2019; Zhou et al. 2019). In rodent models, *Shank3* knockout mice showed enhanced pitch discrimination (Rendall et al. 2019). Although these findings suggest possible links between *SHANK3* and the atypical auditory processing in ASD, the frequencies of auditory stimuli used in the rodent studies (10–48 kHz) ranged far above the frequencies to which the human auditory system is sensitive (1–4 kHz) (Grothe and Pecka 2014). There has been little evidence that *Shank3* mutations causally lead to atypical (enhanced in particular) processing of auditory stimuli within human-sensitive frequencies, leaving it an open question regarding a possible mechanistic link between *SHANK3* mutations and the auditory hypersensitivity observed in ASD patients.

The current work addressed this issue by recording electrocorticograms (ECoGs) to tones in *Shank3* mutant and wild-type dogs. Dog is a credible species for investigating particular aspects of the evolution of human sociocognition in comparative neuroscience. Dogs have acquired the ability to engage in acoustic communication with humans during the process of domestication (Andics et al. 2016). Dogs also exhibit a range of sociocognitive skills that

Received: April 5, 2023. **Revised:** July 26, 2023. **Accepted:** July 27, 2023

share key behavioral and functional characteristics with humans (Bunford et al. 2017). Moreover, dogs and humans are sensitive to sounds of a similar frequency range and dogs process acoustic cues from human or dog vocalizations in overlapping auditory brain regions (Andics et al. 2014). Our recent study showed that *Shank3* mutant dogs generated by CRISPR/Cas9 editing exhibited social withdrawal and elevated anxiety mimicking the clinical manifestations of ASD patients (Tian et al. under review). The current study further employed the *Shank3* mutant dogs as a model to examine possible relationships between *Shank3* mutations and atypical auditory processing.

We recorded ECoGs from *Shank3* mutant and wild-type dogs in an "oddball" paradigm in which deviant tones of different frequencies or probabilities were presented along with other tones in a repetitive stream (standards). Studies of ASD patients (relative to controls) using this paradigm found larger amplitudes of event-related potentials (ERPs) to infrequent pitch changes in tones and vowels within 200 ms after onsets of auditory stimuli (Lepistö et al. 2005; Roberts et al. 2011). To find a potential role of *Shank3* in auditory processing, we compared ECoGs to deviant tones with varying frequencies (Experiment 1) and probabilities (Experiment 2) to test whether neural responses to deviant tones were enhanced or more sensitive to variations of deviant frequencies in *Shank3* mutants compared with wild-type dogs. Our results showed larger amplitudes of early neural responses to and increased sensitivity to varations of frequencies of deviant tones in *Shank3* mutant compared with wild-type dogs. These findings suggest new genetic and neural mechanisms underlying the abnormal auditory processing in ASD patients.

Materials and methods

Subjects

Five wild-type Beagle dogs from Sinogene Ltd (Beijing, China) and five *Shank3* heterozygous mutant dogs (all males aged from 1 to 3 years) were tested in all experiments. Two mutant dogs were −496 bp/+ and three were −483+7 bp/+ (−496 bp and −483+7 bp refer to two specific indels in exon 21 of the *Shank3* gene where there are deletions of 496 and 483 base pairs together with an additional insertion of 7 base pairs, respectively. + after the slash means a wild-type copy of the gene). These mutations generate frameshifts and truncated proteins disrupting the ANK domain and proline-rich domain of Shank3. All mutant dogs showed a similarly reduced level of Shank3 protein and similar autism-like social deficits, including social withdrawal, elevated anxiety, and reduced social interactions with humans (Tian et al. under review). Each dog was housed in a separate cage and maintained on a 12-hour light/12-hour dark cycle with lights on at 7:00 am. The dogs were fed with canine food (Keao Ltd, Beijing, China) twice daily from 08:00 to 10:00 and 15:30 to 17:00. No animal was sacrificed in this study. All experimental protocols (AP2022001) were approved by the Institutional Animal Care Committee of the Institute of Genetics and Developmental Biology, Chinese Academy of Sciences, and all procedures were carried out in accordance with the institutional policies for the Care and Use of Laboratory Animals.

Experimental procedures for ECoG recording

Surgery for electrode implantation was performed under general anesthesia and strictly sterile conditions. The subject dogs were anesthetized by simultaneous administration of dexmedetomidine hydrochloride (5 μg/kg, intramuscular), Zoletil 50 (1 mg/kg, intramuscular), and propofol (5 mg/kg, intravenous), as previously described (Grimm et al. 2011). Heart rate, blood pressure, body temperature, SpO2 (peripheral capillary oxygen saturation), ETCO2 (end-tidal carbon dioxide), and reflex response to noxious stimulation were monitored throughout surgery by an electrocardiogram monitor (Jieruitai, Changsha, China) to adjust the dose of isoflurane accordingly. We implanted customized 32-channel ECoG arrays (Kedou, Suzhou, China) in the epidural space; each electrode was made of 2.0 mm diameter copper and gold disc with an inter-electrode distance of 5 mm. Electrodes were placed to cover most of the lateral surface of the right hemisphere including the frontal, motor, parietal, temporal, and occipital cortices because neural responses to novel stimuli are stronger in the right hemisphere of the brain (Rinne et al. 2000; Naatanen et al. 2007). The position coordinates of recording electrodes were determined based on the combination of pre-acquired magnetic resonance images and postoperative computer tomography images.

A classical auditory-frequency oddball paradigm following previous reports (Sams et al. 1985; Gil-da-Costa et al. 2013) was employed in this study. Auditory stimuli were generated using the software Praat (http://www.praat.org/) and delivered by audio speakers (Philips, Shanghai, China) in a sound-attenuating room. Each acoustic stimulus was a pure sinusoidal tone of 100 ms (10 ms rise/fall) duration with 80 dB SPL intensity. Inter-stimulus interval varied randomly from 600 to 800 ms. Intervals between tones were varied to prevent predictability of the acoustic events. Psychtoolbox-3 (Brainard 1997) was used to control the presentation of auditory stimuli.

ECoG recordings were performed in subjects with restricted moving in square fences (0.9 m × 0.9 m). We recorded one ECoG session per day, including 6 blocks (3 blocks in each experiment) in Experiments 1 and 2 in a random order. The probability or frequency of deviant stimuli were specific for each block. In Experiment 1, 1,100, 1,200, or 1,500 Hz deviant tones with a probability of 20% were presented among 1,000 Hz standard tones. In Experiment 2, 1,500 Hz deviant tones with a probability of 50, 20, or 10% were delivered among 1,000 Hz standard tones. These frequencies were selected based on the overlapping frequency ranges in dogs and humans (Barber et al. 2020) and those used in the previous reports on monkeys and humans (Gil-da-Costa et al. 2013; Lee et al. 2017). Each block consisted of 500 stimuli including 100 deviant stimuli in Experiment 1. To obtain an equal number of deviant stimuli (n = 100) in different conditions in Experiment 2, we delivered 200, 500, and 1,000 stimuli with 50, 20, and 10% of devienat tones in each block, respectively. There were 45 sessions (6 blocks per session, one session per day, 9 sessions per dog) performed on five wild-type and five *Shank3* mutant dogs for statistical analysis. The numbers of trials for statistical analysis of each condition are presented in Table S1.

ECoG data acquisition and analysis

Zeus data acquisition systems (Zeus, Nanjing, China) were used to record ECoG signals with a sampling rate of 1 kHz. ECoG data analyses were performed in MATLAB version 2020b (Mathworks Inc., Natick, MA) and the EEGLAB toolbox (Delorme and Makeig 2004). During pre-processing, those signals were re-referenced using a common average referencemontage, and band-pass filtered from 0.1 to 30 Hz. Neural responses specific to deviant tones were quantified as the differential responses to deviant vs. standard tones over frontal/central electrodes (channels 9, 11, 13, 19, 21, 23, 25, and 27; shown in red box in Fig. 2) and temporal electrodes (channels 1, 2, 4, 6, 8, and 10; shown in green box in Fig. 2) in all experiments. We segmented datasets from −100 to 500 ms

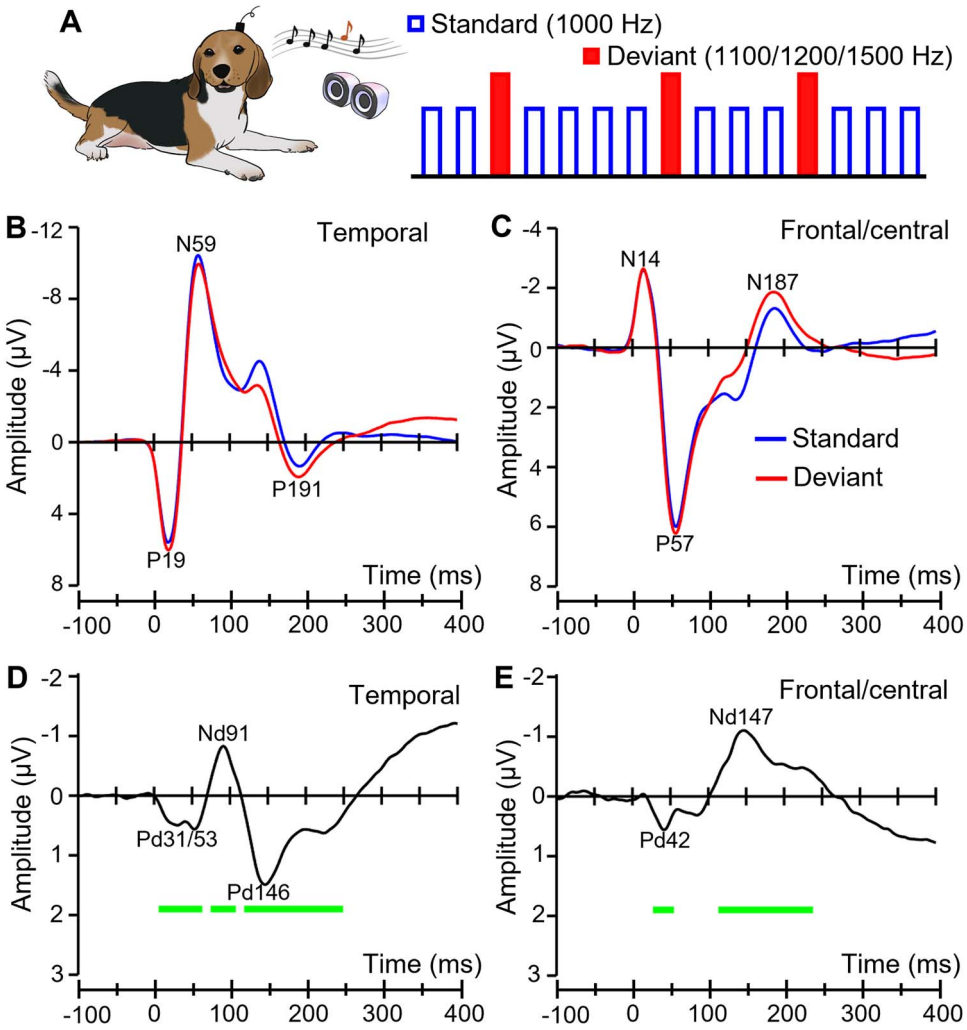

Fig. 1. Neural response to deviant stimuli at varied frequencies in dogs. (A) Illustration of the auditory oddball paradigm used in this study. The stimulus sequence consisted of repeated 1,000 Hz standard tones (blue box) and rare deviant tones (red bar)with varied frequencies (1,100, 1,200, or 1,500 Hz). (B) The temporal ERPs averaged from all deviants of all frequencies (1,100/1,200/1,500 Hz) in both groups (wild types and mutants). (C) Grand averaged ERPs to all deviants of all frequencies in frontal/central telectrodes. (D) Differential neural responses to deviant (vs. standard) stimuli at the temporal electrodes, including Pd31/53 at 11–59 ms and Nd91 at 79–103 ms, followed by Pd146 at 126–166 ms. (E) Pd42 (32–50 ms) and Nd147 (123–245 ms) response to deviant tones in frontal/central electrodes. Green lines in D and E marked time windows in which deviant tones evoked significant responses (point-by-point paired *t*-tests, $P < 0.01$, FDR corrected).

relative to the onset of stimuli. To avoid artifacts arising from differences in the number of standard ($n = 400$) and deviant ($n = 100$) trials, we selected all deviant tones ($n = 100$) and the standard tones immediately preceding the deviants ($n = 100$). Both standard and deviant epochs were applied to baseline corrections from −100 to 0 ms. After the baseline correction, an automatic data cleaning procedure was performed. We first cleaned epochs for all electrodes with abnormal trends (*rejtrend* function: slope > 100 μV with $R^2 > 0.5$). Next, epochs over frontal/central and temporal electrodes containing a voltage difference of more than 50 μV between sample points, a voltage difference exceeding 150 μV within a trial, or a maximum voltage difference less than 0.5 μV within 100 ms intervals were automatically rejected.

Statistical analysis

Neural responses to tones in each trial were averaged to obtain grand-averaged ERPs to tones in different conditions. To quantify the neural response specific to deviant tones, we calculated difference waves by subtracting the averaged ERPs to standard tones from the averaged ERPs to deviant tones. The difference waves were calculated to examine neural responses specific to deviant tones of each frequency (1,100/1,200/1,500 Hz, Expeirment 1) and each probability (50, 20, and 10%, Expeirment 2) from the frontal/central and temporal electrodes in both subject groups (wild types and mutants). These difference waves were further analyzed by conducting point-by-point paired *t*-tests with false discovery rate (FDR) corrections. The mean amplitudes of the difference waves components were averaged from time windows centered around the peak latency ±10 or 20 ms (Luck and Gaspelin 2017). To compare the difference waves between wild type and *Shank3* mutant dogs, the mean amplitudes of the difference waves were subjected to a two-way repeated measures analysis of variance (ANOVAs) with Frequency (1,100, 1,200, or 1,500 Hz, Expeirment 1) or Probability (50, 20, or 10%, Experiment 2) of deviant tones as a within-subjects factor and Group (*Shank3* mutant vs. wild-type dogs) as a between-subjects factor. Greenhouse–Geisser epsilon corrections were applied to adjust the degree of freedom when the sphericity assumption was violated. Post-hoc comparisons were corrected using the Bonferroni procedure. The summary of statistical analysis results is presented in Table S2.

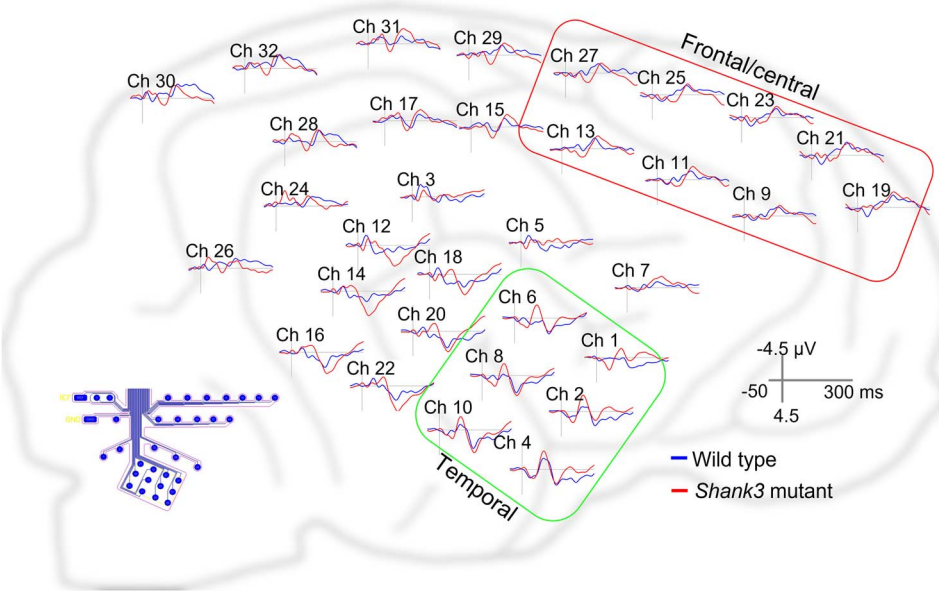

Fig. 2. Maximal differences in ERPs between wild-type and mutant dogs observed in the temporal electrodes. Graphs depict difference waves (obtained by subtracting the ERPs to standard from those to deviant stimulus) in wild-type (blue line) and *Shank3* mutant (red line) dogs. The frontal/central and temporal electrodes were indicated by red and green box, respectively. The electrodes array is shown at the bottom left. Ch, channel.

Results

Neural responses specific to deviant tones in dogs

In Experiment 1, we recorded ECoG signals from wild-type and *Shank3* mutant dogs using a classic auditory oddball paradigm with infrequent 1,100, 1,200, or 1,500 Hz deviants at 20% probability embedded in a rhythmic stream of repeatedly occurring 1,000 Hz standard pure tones (Fig. 1A). To avoid biased evaluation of neural responses specific to deviant tones, we first calculated grand-averaged ERPs to standard and deviant tones by averaging ECoG signals to deviant tones of all frequencies (1,100/1,200/1,500 Hz) in both subject groups (wild types and mutants). The ERPs observed at the temporal electrodes were characterized by an early positive deflection at 9–29 ms peaking at 19 ms (P19), followed by a negative deflection at 49–69 ms (N59), and a late positive deflection at 131–251 ms (P191), as illustrated in (Fig. 1B). ERP components at the frontal/central electrodes included an early negative deflection at 4–24 ms (N14), a positive deflection at 47–67 ms (P57), and a late negative deflection at 127–247 ms (N187), as illustrated in (Fig. 1C).

Neural responses specific to deviant tones were identified by calculating difference waves (ERPs to deviant tones minus those to standard tones) and analyzed by conducting point-by-point paired *t*-tests to compare ERPs for deviant vs. standard tones at 0–400 ms. The first positive response (Pd53) in *Shank3* mutant dogs (Fig. 3D) was delayed compared with that (Pd31) observd in wild-type dogs (Fig. 3B). A paired *t*-test revealed three neural responses specific to deviant tones, including an early positive response peaking at 31/53 ms (11–59 ms) and a negative response (Nd91 at 79–103 ms), followed by a late positive response (Pd146 at 123–245 ms) at the temporalelectrodes ($P < 0.01$, all FDR corrected; Fig. 1D). The Pd31/53, Nd91, and Pd146 showed the largest ampalitudes at the temporal electrodes compared with other electrodes. Neural response specific to deviant tones at the frontal/central electrodes were characterized by a positive response Pd42 (32–50 ms) and a negative response Nd147 (118–234 ms) (Fig. 1E). In the following analysis, we focoused on the difference in neural responses specific to deviant tones (i.e. difference waves, Fig. 2) between wild-type and mutant dogs.

Enhanced early neural responses to deviant tones in *Shank3* mutants

Figure 3A–D show ERPs at the temporal electrodes in response to standard tones and deviant tones of different frequencies in Experiment 1. To compare neural processing of deviant tones between *Shank3* mutant and wild-type dogs, we calculated the mean amplitudes of Pd31/53 (21–41 ms in wild types, 43–63 ms in mutants), Nd91 (81–101 ms), and Pd146 (126–166 ms) to deviant tones of different frequencies. The amplitudes of each neural response were subjected to ANOVAs with Deviant frequency (1,100, 1,200, vs. 1,500 Hz) as a within-subjects factor and Group (*Shank3* mutant vs. wild-type dogs) as a between-subjects factor. ANOVA of the mean Pd31/53 amplitudes showed a significant interaction of Deviant frequency × Group (two-way ANOVA, $F_{(2, 176)} = 3.748$, $P = 0.027$, $\eta 2$ $P = 0.041$, 90% confidence interval (CI) = 0.003–0.092), indicating distinct sensitivity of the mean Pd53 amplitudes in response to deviant tones of different frequeicnes in *Shank3* mutant and wild-type dogs. Further analyses found that a higher frequency of deviant (vs. standard) tones elicited a greater Pd53 response in *Shank3* mutant dogs (main effect of frequency: $F_{(2, 87)} = 5.324$, $P = 0.007$, $\eta 2$ $P = 0.109$, 90% CI = 0.019–0.205) but not in wild-type dogs ($F_{(2, 87)} = 1.641$, $P = 0.2$, $\eta 2$ $P = 0.036$, 90% CI = 0–0.106; Fig. 3E).

The ANOVA of mean Nd91 amplitude revealed a significant main effect of frequency ($F_{(2, 176)} = 3.138$, $P = 0.047$, $\eta 2$ $P = 0.034$, 90% CI = 0011–0.082), indicating larger Nd91 amplitudes to deviant tones with higher frequencies (Fig. 3F). In addition, there was a significant main effect of Group ($F_{(1, 88)} = 11.746$, $P = 0.001$, $\eta 2$ $P = 0.118$, 90% CI = 0.032–0.225; Fig. 3F) due to a larger Nd91 amplitude in *Shank3* mutant than wild-type dogs. However, there was no interaction of Deviant frequency × Group ($F_{(2, 176)} = 1.332$, $P = 0.267$, $\eta 2$ $P = 0.015$, 90% CI = 0–0.049). The ANOVA of the mean Pd146

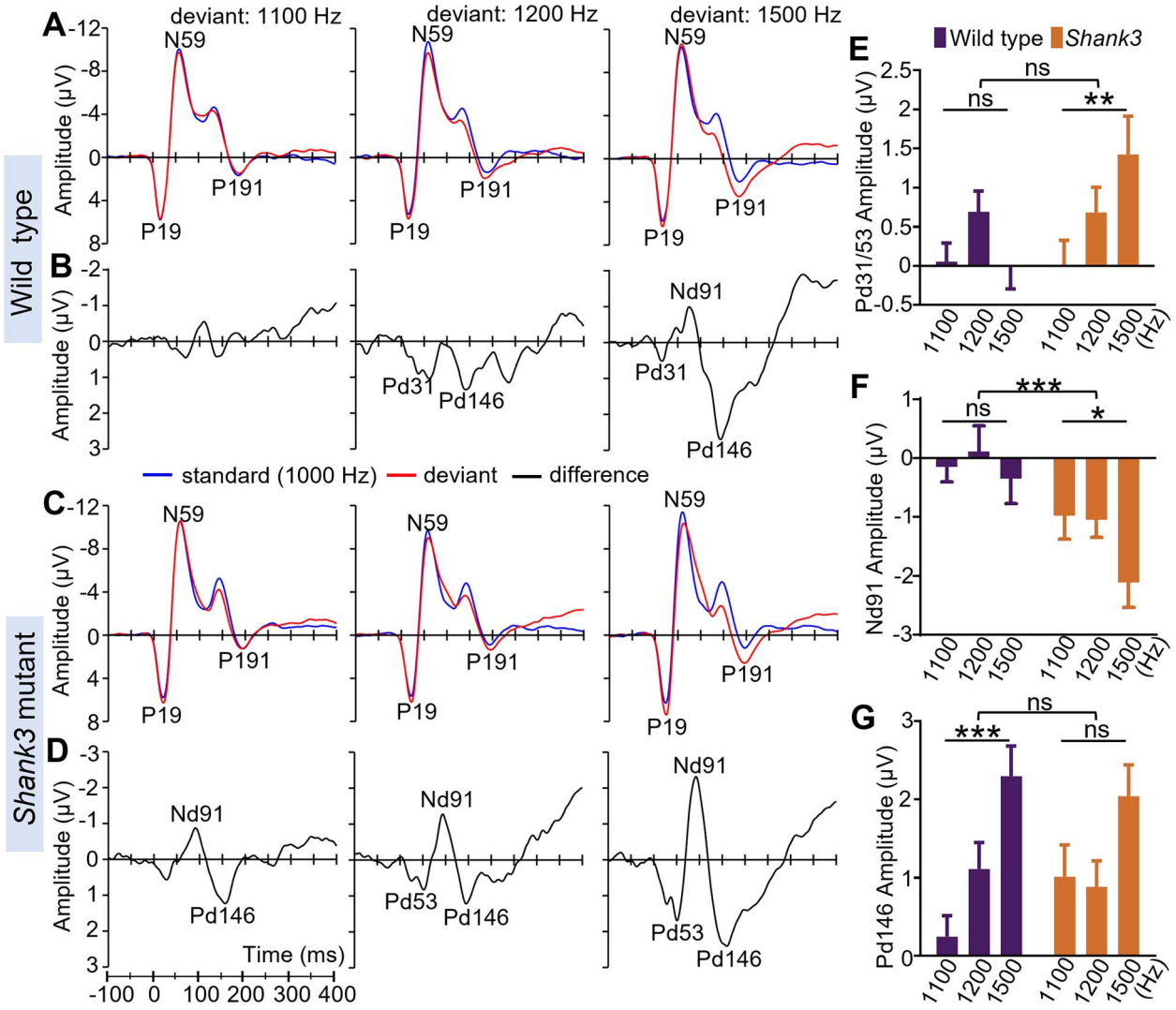

Fig. 3. Neural responses to deviant tones are enhanced in *Shank3* mutant dogs. (A) Grand averaged ERPs to 1,000 Hz standard stimuli (blue line) and deviant stimuli (20% probability, red line) from the temporal electrodes in wild-type dogs. The deviant frequency varied among 1,100, 1,200, and 1,500 Hz. Both deviant and standard tones evoked an early positivity P19 followed by an N59 and a P191. (B) Differential neural responses to deviant (vs. standard) stimuli in wild-type dogs. These include Pd31, Nd91, and Pd146. (C) Grand averaged ERPs to standard stimuli (blue line) and deviant stimuli (red line) were recorded from the temporal electrodes in *Shank3* mutant dogs. (D) Differential neural activities in response to deviant (vs. standard) tones in *Shank3* mutant dogs. (E–G) Early responses (Pd53 and Nd91), but not late response Pd146, showed hypersensitivity to deviant frequencies in *Shank3* mutants than wild-type dogs. Data are represented as mean ± SEM; $^{*}P < 0.05$, $^{**}P < 0.01$, $^{***}P < 0.001$ by two-way ANOVA.

amplitudes only revealed a significant main effect of Deviant frequency ($F_{(2,176)} = 11.134$, $P < 0.001$, $\eta 2$ $P = 0.112$, 90% CI = 0.044–0.182; Fig. 3G), suggesting larger Pd146 amplitudes in response to deviant tones with higher frequencies in both subject groups. These results uncovered enhanced neural responses to deviant tones and greater sensitivity of neural responses to deviant frequencies in the early stage of auditory processing in *Shank3* mutants compared with wild-type dogs.

Similar analyses were conducted on the mean Pd42 and Nd147 amplitudes at the frontal/central electrodes (Fig. 4A–F). Only the ANOVA of the mean Nd147 (127–167 ms) amplitudes showed a significant main effect of Devient frequency ($F_{(2,176)} = 6.94$, $P = 0.001$, $\eta 2$ $P = 0.073$, 90% CI = 0.019–0.135), suggesting increased Nd147 amplitudes to deviant tones with higher frequencies in both subject groups. This effect, however, did not differ significantly between *Shank3* mutant and wild-type dogs ($F_{(2,176)} = 0.091$, $P = 0.909$, $\eta 2$ $P = 0.001$, 90% CI = 0–0.006).

Enhanced early neural responses to deviant tones in *Shank3* mutant than wild-type dogs are independent of deviant probability

In Experiment 2 we further investigated whether the enhanced early neural responses to deviant tones in *Shank3* mutants compared with wild-type dogs were independent of the probability of deviant tones. We recorded ECoG signals from wild-type and *Shank3* mutant dogs in response to standard (1,000 Hz) and deviant (1,500 Hz) tones under three conditions in which the probability of deviant stimuli varied (50, 20, and 10%; Fig. 5). Similarly, we first calculated grand-averaged ERPs to standard and deviant tones by averaging ECoG signals to deviant tones of all probabilities (50, 20, and 10%) in both subject groups (wild type and mutant dogs). The ERPs at the temporal electrodes were characterized by an early positive deflection P20 (10–30 ms), following by a negative deflection N58 (48–68 ms), and a late positive deflection P192 (132–252 ms), as shown in (Fig. 5A). ERPs at the frontal/central

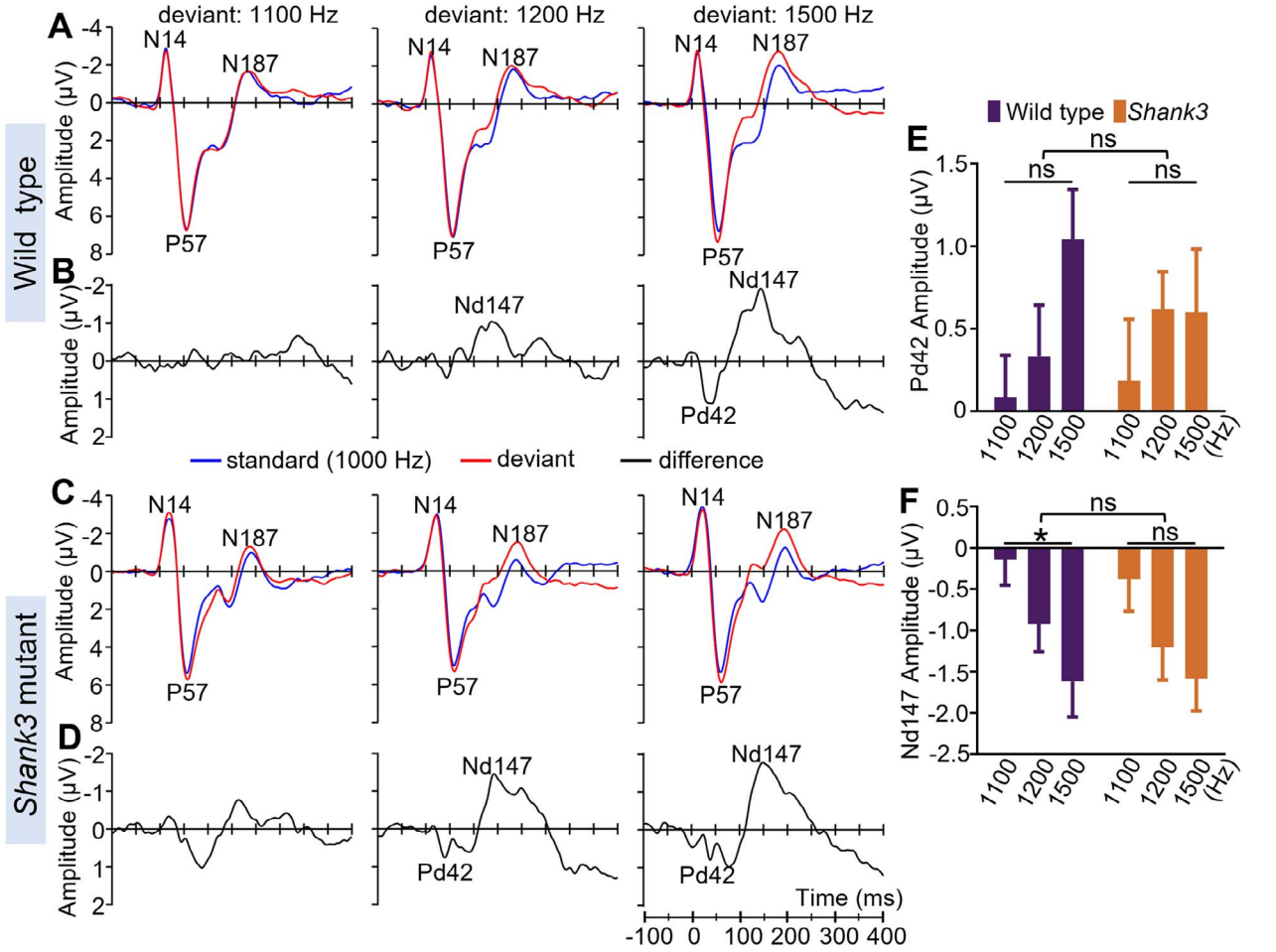

Fig. 4. Neural responses to deviant tones at the frontal/central electrodes in *Shank3* mutant dogs. (A,C) grand averaged ERPs in response to standard tones (blue line) and deviant tones (red line) from the frontal/central electrodes in wild-type (A) and *Shank3* mutant (C) dogs. Both deviant and standard tones evoked an early negativity N14, a positivity P57 and a long-latency negativity N187 under deviant frequency varied among 1,100, 1,200, and 1,500 Hz. (B, D)differential neural responses to deviant (vs. standard) stimuli in wild-type (B) and *Shank3* mutant (D) dogs, evidenced by Pd42 and Nd147. (E, F) no significant difference in Pd42 andNd147 repsonses between wild-type and mutant dogs. Data are represented as mean ± SEM; *$P < 0.05$ by two-way ANOVA.

electrodes consisted of a negative N15 (5–25 ms), followed by P56 (46–66 ms) and late N186 (126–246 ms) (Fig. 5B). Point-by-point paired *t*-tests identified three neural responses to deviant and standard tones, including an early Pd16/55 (4–24 ms in wild types, 52–58 ms in mutants), a negative Nd86 (71–108 ms), and a positive Pd154 (122–276 ms) at the temporal electrodes (Fig. 5C). Similarly, Pd37 (24–53 ms), Pd77 (67–87 ms), and Nd154 (134–174 ms) were observed at the frontal/central electrodes (Fig. 5D).

We conducted ANOVAs of the mean amplitudes of Pd16/55 (6–26 ms in wild types, 45–65 ms in mutants), Nd86 (76–96 ms) and Pd154 (134–174 ms) at the temporal electrodes with Probability (50, 20, and 10%) as a within-subjects factor and Group (*Shank3* mutants vs. wild-type dogs) as a between-subjects factor (Fig. 6A–G). We found the mean Pd16/55 and Nd86 amplitudes showed no significant main effect of Probability (Pd16/55: $F_{(2,176)} = 1.44$, $P = 0.239$, $\eta 2$ $P = 0.016$, 90% CI = 0–0.052; Nd86: $F_{(2,176)} = 0.98$, $P = 0.376$, $\eta 2$ $P = 0.011$, 90% CI = 0–0.042), but ANOVA of the mean Pd16/55 and Nd86 amplitudes revealed significant main effects of Group (Pd16/55: $F_{(1,88)} = 5.417$, $P = 0.022$, $\eta 2$ $P = 0.058$, 90% CI = 0.004–0.15; Nd86: $F_{(1,88)} = 11.176$, $P = 0.001$, $\eta 2$ $P = 0.113$, 90% CI = 0.029–0.219; Fig. 6E, F), indicating larger Pd55 and Nd86 amplitudes in *Shank3* mutant than wild-type dogs. ANOVAs of the mean Pd154 amplitudes revealed a significant main effect of Probability ($F_{(2,176)} = 11.158$, $P < 0.001$, $\eta 2$ $P = 0.113$, 90% CI = 0.015–0.123, Fig. 6G), as the Pd154 amplitudes increased to deviant tones with lower probabilities. In addition, decreased Pd154 amplitudes were found in mutant dogs compared with wild types (main of group, $F_{(1,88)} = 5.165$, $P = 0.025$, $\eta 2$ $P = 0.055$, 90% CI = 0.004–0.147, Fig. 6G). However, the effects of the interaction of Probability × Group on neural responses did not significantly differ between *Shank3* mutants and wild-type dogs ($P = 0.696$, 0.913, and 1.194 for Pd16/55, Nd86, and Pd154 interaction of Probability × Group, respectively).

ERPs at the frontal/central electrodes in response to standard tones and deviant tones of different probabilities are shown in (Fig. 7A–D). The ANOVA of the mean Pd37 and Pd77 amplitudes at the frontal/central electrodes showed significant main effect of Group ($F_{(1,88)} = 6.685$ and 6.682, $P = 0.011$ and 0.011, $\eta 2$ $P = 0.071$ and 0.171, 90% CI = 0.009–0.167 and 0.009–0.167; Fig. 7E, F), indicating smaller Pd37 and larger Pd77 amplitudes in *Shank3* mutant than wild-type dogs. ANOVAs of the mean Nd154 amplitudes at the frontal/central electrodes did not show any significant effect ($P = 0.315$, 0.684, and 0.121 for main effect of Probability, Group, and Probability × Group interaction, respectively) (Fig. 7G). The results in Experiment 2 provide evidence for greater early neural responses to deviant tones in *Shank3* mutants than in

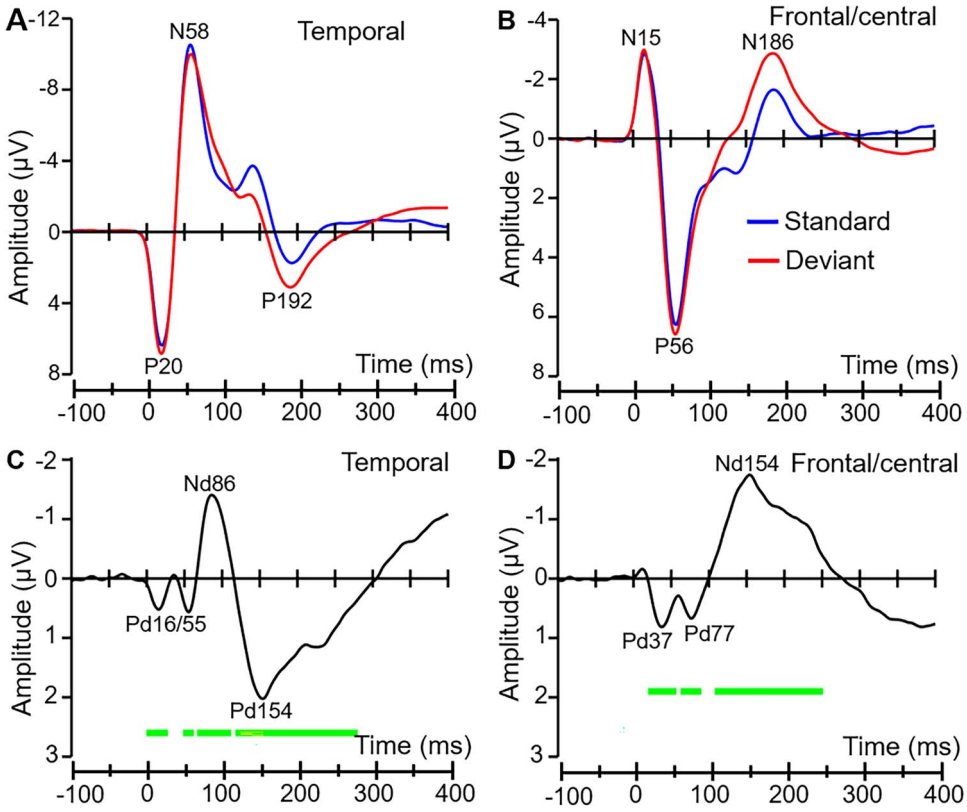

Fig. 5. Neural response to deviant stimuli with varied probability of deviants in dogs. (A, B) Grand averaged ERPs to deviant tones in different probability conditions (50, 20, and 10%) of both wild-type and mutant groups, at temporal (A) and frontal/central (B) electrodes. (C, D) Results of point-by-point paired *t*-tests identified differential neural responses to deviant (vs. standard) stimuli, including Pd16/55 at 4–24 and 52–58 ms and Nd86 at 71–108 ms, followed by Pd154 at 122–276 ms at the temporal electrodes (C), and Pd37 at 24–53 ms, Pd77 at 67–86 ms, and Nd154 at 112–247 ms at the frontal/central electrodes (D). Green lines in C and D marked time windows in which deviant tones evoked significant neural responses (point-by-point paired *t*-tests, $P < 0.01$, FDR corrected).

wild-type dogs regardless of the variation of probabilities of deviant tones.

Discussion

The present study investigated whether *Shank3* mutations cause ASD-like atypical auditory processing by quantifying neural responses to deviant tones using ECoG in wild-type and *Shank3* mutant dogs. ECoG signals specific to deviant tones were identified by calculating difference waves of ECoG signals to deviant (vs. standard) tones with variations of deviant frequencies (Experiment 1) and probability (Experiment 2). Comparisons of the neural responses specific to deviant tones in the two subject groups allowed us to examine the effect of *Shank3* mutations on neural activities involved in auditory processing in a dog model.

Our ECoG results revealed three successive neural responses to deviant tones at the temporal electrodes, including an early positive response Pd31 and a negative response Nd91, followed by a late positive response Pd146, and the Pd42 and Nd147 at the frontal/central electrodes in wild-type dogs. The early neural response (i.e. Pd31) to deviant tones started at about 13 ms and peaked around 30 ms after tone onset. Previous animal studies reported similar early neural responses to novel tones in rats (0–50 ms; Lee et al. 2018), cats (25–50 ms; Pincze et al. 2002), and monkeys (10–48 ms; Gil-da-Costa et al. 2013), different from that in humans (100–250 ms; Naatanen et al. 2001, 2007). The early neural responses to deviant tones observed in our work peaked later than the brainstem auditory evoked potentials that usually occur within 10 ms after stimulus onset in dogs (Strain et al. 1991; Meij et al. 1992) but in a time window of middle-latency auditory-evoked potentials recorded in acepromazine-sedated dogs (Murrell et al. 2004). In addition, ECoG signals at the temporal and frontal/central electrodes (e.g. temporal Pd146 and frontal/central Nd147) showed opposite polarities in a similar time window, suggesting possible sources of the ECoG signals specific to deviant tones in the auditory cortex.

More importantly, our ECoG results unraveled two patterns of distinct neural responses specific to deviant tones in *Shank3* mutant and wild-type dogs. First, while the amplitudes of the two neural responses (Nd91/Pd146) in Experiment 1 increased to deviant tones with higher frequencies in both subject groups, the early response (Pd53) was sensitive to deviant frequencies only in *Shank3* mutant dogs. Spatial mapping of frequency selectivity of neuronal responses in the auditory cortex has been established in different species (Schreiner et al. 2000), including dogs (Tunturi 1962). There are separate neuron clusters along the tonotopic or spectral decomposition axis that respond selectively to preferred frequencies (Merzenich and Schreiner 1992; Schreiner et al. 2000; Petkov et al. 2004). Our findings suggest that *Shank3* mutations might influence neural responses to tone frequencies at an early stage of auditory processing in the primary auditory cortex. Second, we found that *Shank3* mutants compared with wild-type dogs showed larger amplitudes of the Nd91 neural response to deviant tones in Experiment 1 and larger amplitudes of both the Pd55 and Nd86 responses to deviant tones in Experiment 2. Moreover, the enhanced neural responses to deviant tones in *Shank3* mutant (vs.

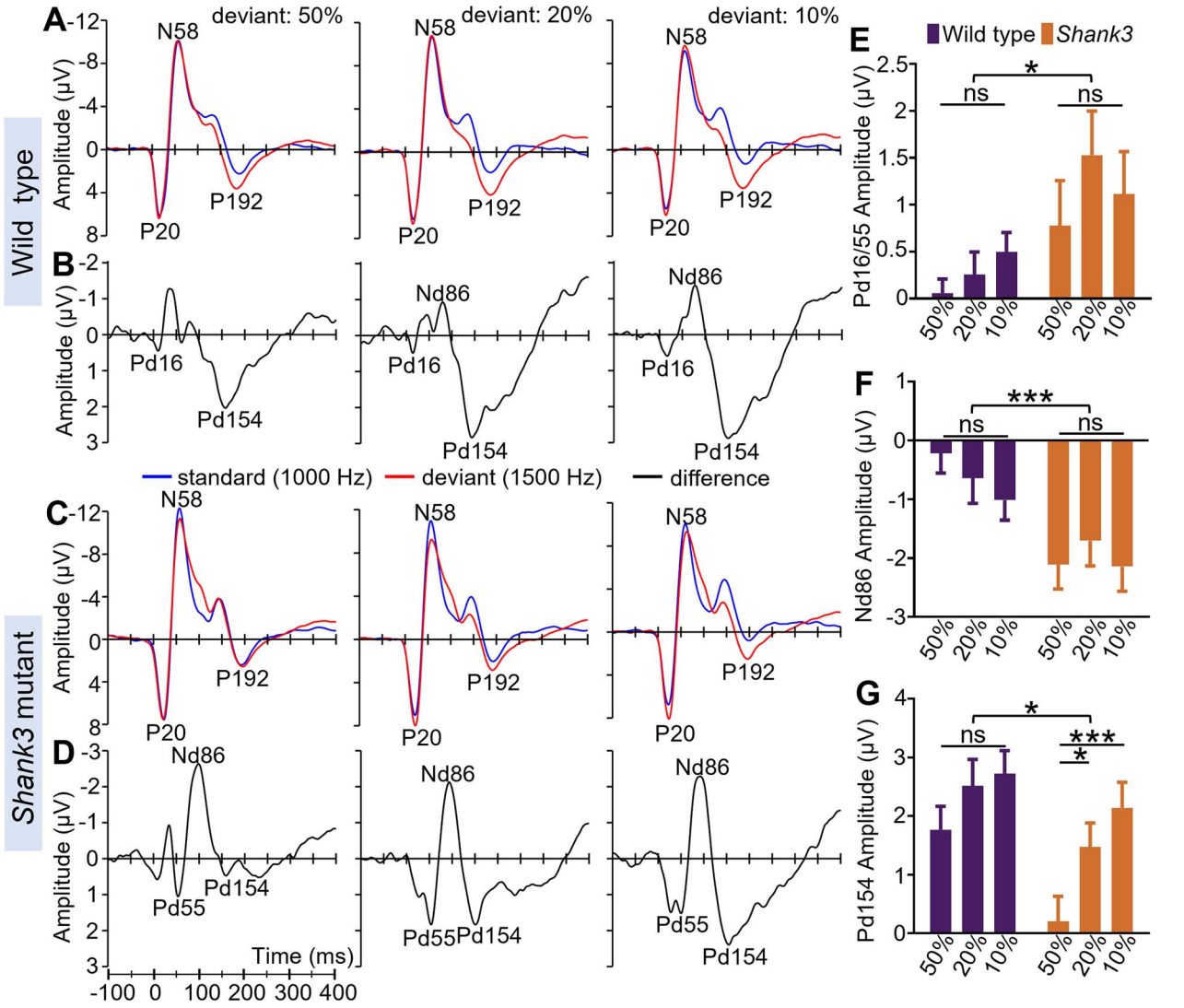

Fig. 6. Enhanced early neural responses to deviant tones in *Shank3* mutant dogs independent of deviant probability. (A, C) grand averaged ERPs in response to 1,000 Hz standard tones (blue line) and 1,500 Hz deviant tones (red line) from the temporal electrodes in wild-type (A) and *Shank3* mutant (C) dogs. The deviant probability varied among 50, 20, or 10%. Both deviant and standard tones evoked an early positivity P20 at 10–30 ms followed by a negativity N58 at 48–68 ms and a long-latency positivity P192 at 132–252 ms. (B, D) Neural responses to deviant tones in wild-type (B) and *Shank3* mutant (D) dogs. The response include Pd16/55, Nd86, and Pd154. (E–G) Early neural response (Pd16/55 and Nd86) showed significant difference between wild-type and mutant dogs.

wild-type) dogs were evident regardless of deviant frequency or probability varied in the stream of auditory stimuli. These results provide experimental evidence supporting that *Shank3* mutations result in enhanced early neural responses to deviant tones in dogs.

Electroencephalography (EEG) studies of humans using scalp electrodes showed electrophysiological responses to deviant tones as early as 100 ms after stimulus onset in humans (100–250 ms), which are denoted as mismatch negativity (MMN) with a source in the auditory cortex (Naatanen et al. 2007). There is also evidence that MMN amplitudes in humans are sensitive to deviant frequency and probability, as there are increased MMN amplitudes to deviant stimuli with a higher frequency or a lower probability (Sams et al. 1985; Sato et al. 2000; Naatanen et al. 2007). Comparisons of the electrophysiological and pharmacological properties suggest a homology between MMN in humans and MMN-like responses in animals (Shiramatsu and Takahashi 2021). The Nd86 and Nd91 observed in dogs seem to be homologous to MMN in humans. Unlike previous ERP studies of dogs that reported a negative deflection in response to deviant tones at 160–200 ms in dogs (Howell et al. 2012), we found earlier Nd86 and Nd91 responses to deviant tones, similar to other animal studies that found MMN-like repsonses within 150 ms after stimulus onset (e.g. at 61–75 ms in cats, Pincze et al. 2002; at 48–120 ms in monkeys, Gil-da-Costa et al. 2013). Increased MMN amplitudes and delayed latencies to tone-frequency deviants were observed in ASD patients relative to the typically developed controls (Roberts et al. 2011; Matsuzaki et al. 2019). Larger MMN amplitudes were also observed in children with autism who showed auditory hypersensitivity and superior pitch-processing abilities (Lepistö et al. 2005). Based on the findings of abnormal MMN in ASD patients who exhibit aberrant processing of various low-level perceptual features of sounds (e.g. loudness and frequency; O'Connor 2012), one may hypothesize a causal relationship between *SHANK3* mutations and enhanced processing of low-level perceptual features of sounds. Our ECoG findings that *Shank3*

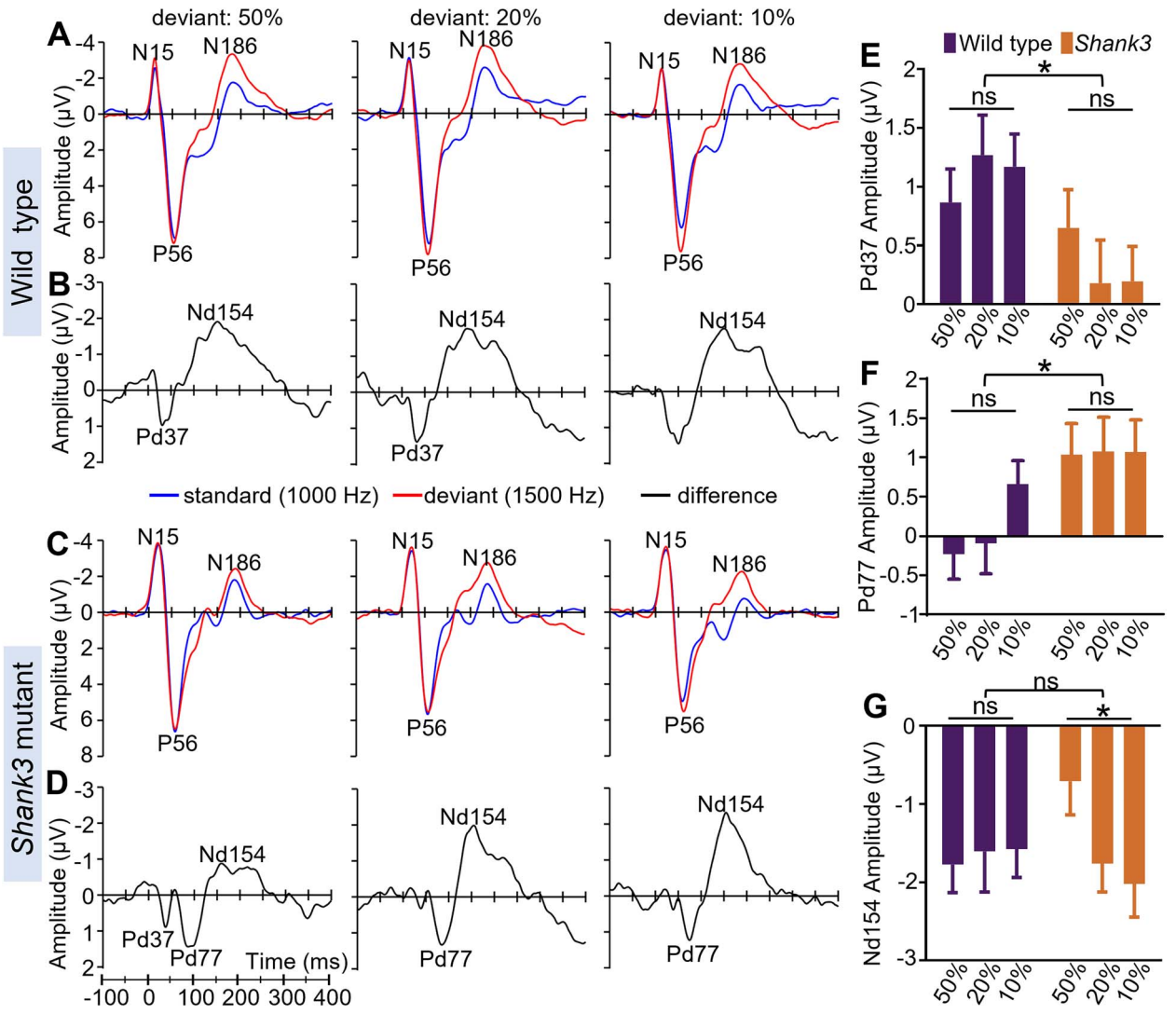

Fig. 7. Enhanced neural responses to deviant tones in frontal/central electrodes in *Shank3* mutant dogs. (A, C) Grand averaged ERPs in response to standard tones (blue line) and deviant tones (red line) from frontal/central electrodes in wild-type (A) and *Shank3* mutant (C) dogs. Both standard and deviant tones elicited an early negativity N15 at 5–25 ms followed by a positivity P56 at 46–66 ms and a long-latency positivity N186 at 126–246 ms. (B, D) Neural response to deviant tones in wild-type (B) and *Shank3* mutant (D) dogs, including Pd37, Pd77, and Nd154. (E–G) Early neural responses (Pd37 and Pd77) are significantly different between wild-type and mutant dogs. No significant difference in Nd154 (G) was observed between wild types and mutants.

mutations led to enhanced neural sensitivity to frequencies of deviant tones provide experimental evidence supporting this hypothesis.

Because *SHANK3* mutation is one of the most extensively characterized risk factors associated with ASD (Monteiro and Feng 2017), there have been increasing interests in generating animal models, mostly rodent models, with *Shank3* mutations to elucidate the atypical auditory processing in ASD patients (Zhou et al. 2016; Engineer et al. 2018; Rendall et al. 2019; Castro and Monteiro 2022). However, humans use low-frequency sounds for vocal communication, and dogs and humans share a similar sensitivity to sounds of low frequencies (Barber et al. 2020). Besides, dogs are sensitive to segmental cues in speech and are able to process emotional prosody and speech familiarity (Andics et al. 2014; Ratcliffe and Reby 2014; Cuaya et al. 2022). We report in the present study atypical processing of auditory information in *Shank3* mutant dogs, which exhibited deficits in social behavior (Tian et al. under review). The co-occurrence of abnormal sensory perceptual processing and social-cognitive deficits is repeatedly reported in autism (Robertson and Baron-Cohen 2017). The relationship between enhanced auditory processing and social deficits in ASD patients remain unclear, though abnormal auditory processing was observed in ASD patients with language impairments (Roberts et al. 2011) and proposed to predict the severity of autistic traits (Brandwein et al. 2015). Our previous (Tian et al. under review) and current studies showed evidence of social deficits and enhanced neural sensitivity to perceptual features of auditory stimuli in *Shank3* mutant dogs, respectively. One possibility is that enhanced sensory and perceptual processing leads to insensitivity to social information of stimuli and thus results in deficits in social behavior. Alternatively, the atypical auditory processing observed in *Shank3* mutant dogs might be a side effect of social deficits or independent of impaired social behaviors. Indeed, dogs with their ability to process the features of human speech (Andics et al. 2016) provide a compelementary and valuable animal model for studying the relationship between abnormal auditory information processing and social deficits in ASD patients.

Our findings leave open questions regarding the mechanisms that link *Shank3* mutation and ASD-like abnormal responses to deviant tones. Neuroimaging studies of humans have shown evidence that attention enhanced the MMN amplitudes (Alho et al. 1992) and increased neural responses to sounds of broad frequencies in the primary auditory cortex (Petkov et al. 2004). In human ASD patients, specific gene mutations may facilitate focused attention by ignoring contextual information to elevate the sensitivity to low-level perceptual features of auditory stimuli. Whether a similar mechanism exists in *Shank3* mutant dogs can be examined in future research. Although ECoG recordings acquire high-fidelity broadband neuronal signals from an entire cortical hemisphere, the recording technique limited the sample size. In addition, our study collected ECoG data from males only to avoid potential confounds of sex differences in the effect of *Shank3* mutations on auditory processing. Our findings contributed to the understanding of the genetic and neural mechanisms underlying ASD that is more common in males than in females (Lord et al. 2020). Further studies should increase sample size and include more subjects of different sexes and ages. Furthermore, the passive hearing paradigm used in the present study did not provide measures of behavioral responses and thus did not allow us to dissect the relationship between behavioral and neural responses to tones in *Shank3* mutant dogs. One possible solution is to track pupil dilation responses that increase to deviant sounds (Marois et al. 2018) and covary with blood oxygenation level dependent activity in human locus coeruleus (Murphy et al. 2014).

In conclusion, our ECoG results unraveled early neural responses to novel sounds in wild-type dogs. Moreover, our ECoG results revealed larger amplitudes of the early neural responses to deviant tones, and more sensitive to varied frequencies in *Shank3* mutant dogs. Our findings provide experimental evidence for the association between *Shank3* mutations and enhanced neural activities underlying the processing of low-level features of sounds. The *Shank3* mutant dogs tested in the present study are expected to facilitate future studies of mechanisms underlying the widespread atypical sensory processing in ASD patients.

Acknowledgments

We thank Dr. Li Hu, Dr. Liping Wang, and Dr. Kun Guo for helpful discussions, Siqi Yuan, Qi Shi, and Xinyong Han for assistance in experiments.

Author contributions

Liang Wu (Formal analysis, Investigation, Writing—original draft), Shuting Mei (Formal analysis, Writing—original draft), Shan Yu (Funding acquisition, Project administration, Supervision, Writing—review and editing), Shihui Han (Conceptualization, Funding acquisition, Project administration, Supervision, Writing—review and editing), Yong Q. Zhang (Conceptualization, Funding acquisition, Project administration, Supervision, Writing—review and editing).

Supplementary material

Supplementary material is available at *Cerebral Cortex* online.

Funding

This work was supported by grants from The National Key Research and Development Program (2019YFA0707100 and 2021ZD0203901 to Y.Q. Z., and 2019YFA0707103 to S.H.), the Strategic Priority Research Program B of the Chinese Academy of Sciences (XDBS1020100 to Y.Q.Z. and XDB32040201 to S.Y.), the National Science Foundation of China (31830036 and 31921002 to Y.Q.Z.), and the Spring City Plan (2022SCP001 to Y.Q.Z.).

Conflict of interest statement: None declared.

Data availability

Data and code are available upon request.

References

Alho K, Woods DL, Algazi A, Naatanen R. Intermodal selective attention. II. Effects of attentional load on processing of auditory and visual stimuli in central space. *Electroencephalogr Clin Neurophysiol*. 1992:82:356–368.

American Psychiatric Association. *Diagnostic and statistical manual of mental disorders*. 5th ed. Arlington, VA: American Psychiatric Publishing; 2013.

Andics A, Gacsi M, Farago T, Kis A, Miklosi A. Voice-sensitive regions in the dog and human brain are revealed by comparative fMRI. *Curr Biol*. 2014:24:574–578.

Andics A, Gabor A, Gacsi M, Farago T, Szabo D, Miklosi A. Neural mechanisms for lexical processing in dogs. *Science*. 2016:353:1030–1032.

Barber ALA, Wilkinson A, Montealegre-Z F, Ratcliffe VF, Guo K, Mills DS. A comparison of hearing and auditory functioning between dogs and humans. *Comp Cogn Behav Rev*. 2020:15:45–94.

Bonnel A, McAdams S, Smith B, Berthiaume C, Bertone A, Ciocca V, Burack JA, Mottron L. Enhanced pure-tone pitch discrimination among persons with autism but not Asperger syndrome. *Neuropsychologia*. 2010:48:2465–2475.

Brainard DH. The Psychophysics Toolbox. *Spat Vis*. 1997:10:433–436.

Brandwein AB, Foxe JJ, Butler JS, Frey HP, Bates JC, Shulman LH, Molholm S. Neurophysiological indices of atypical auditory processing and multisensory integration are associated with symptom severity in autism. *J Autism Dev Disord*. 2015:45:230–244.

Bunford N, Andics A, Kis A, Miklósi Á, Gácsi M. Canis familiaris as a model for non-invasive comparative neuroscience. *Trends Neurosci*. 2017:40:438–452.

Castro AC, Monteiro P. Auditory dysfunction in animal models of autism spectrum disorder. *Front Mol Neurosci*. 2022:15:845155.

Chen JA, Penagarikano O, Belgard TG, Swarup V, Geschwind DH. The emerging picture of autism spectrum disorder: genetics and pathology. *Annu Rev Pathol*. 2015:10:111–144.

Cuaya LV, Hernandez-Perez R, Boros M, Deme A, Andics A. Speech naturalness detection and language representation in the dog brain. *NeuroImage*. 2022:248:118811.

De Rubeis S, Siper PM, Durkin A, Weissman J, Muratet F, Halpern D, Trelles MDP, Frank Y, Lozano R, Wang AT, et al. Delineation of the genetic and clinical spectrum of Phelan-McDermid syndrome caused by SHANK3 point mutations. *Mol Autism*. 2018:9:31.

Delorme A, Makeig S. EEGLAB: an open source toolbox for analysis of single-trial EEG dynamics including independent component analysis. *J Neurosci Methods*. 2004:134:9–21.

Engineer CT, Rahebi KC, Borland MS, Buell EP, Im KW, Wilson LG, Sharma P, Vanneste S, Harony-Nicolas H, Buxbaum JD, et al. Shank3-deficient rats exhibit degraded cortical responses to sound. *Autism Res*. 2018:11:59–68.

Ferri R, Elia M, Agarwal N, Lanuzza B, Musumeci SA, Pennisi G. The mismatch negativity and the P3a components of the auditory event-related potentials in autistic low-functioning subjects. *Clin Neurophysiol*. 2003:114:1671–1680.

Gil-da-Costa R, Stoner GR, Fung R, Albright TD. Nonhuman primate model of schizophrenia using a noninvasive EEG method. *Proc Natl Acad Sci U S A*. 2013:110:15425–15430.

Grimm A, Tranquilli J, Lamont A. *Essentials of small animal anesthesia and analgesia*. 2nd ed. Chichester, West Sussex: Wiley-Blackwell; 2011.

Grothe B, Pecka M. The natural history of sound localization in mammals–a story of neuronal inhibition. *Front Neural Circuits*. 2014:8:116.

Howell TJ, Conduit R, Toukhsati S, Bennett P. Auditory stimulus discrimination recorded in dogs, as indicated by mismatch negativity (MMN). *Behav Process*. 2012:89:8–13.

Lee M, Sehatpour P, Hoptman MJ, Lakatos P, Dias EC, Kantrowitz JT, Martinez AM, Javitt DC. Neural mechanisms of mismatch negativity dysfunction in schizophrenia. *Mol Psychiatry*. 2017:22: 1585–1593.

Lee M, Balla A, Sershen H, Sehatpour P, Lakatos P, Javitt DC. Rodent mismatch negativity/theta neuro-oscillatory response as a translational neurophysiological biomarker for N-methyl-D-aspartate receptor-based new treatment development in schizophrenia. *Neuropsychopharmacology*. 2018:43:571–582.

Lepistö T, Kujala T, Vanhala R, Alku P, Huotilainen M, Naatanen R. The discrimination of and orienting to speech and non-speech sounds in children with autism. *Brain Res*. 2005:1066:147–157.

Lord C, Brugha TS, Charman T, Cusack J, Dumas G, Frazier T, Jones EJH, Jones RM, Pickles A, State MW, et al. Autism spectrum disorder. *Nat Rev Dis Primers*. 2020:6:5.

Luck SJ, Gaspelin N. How to get statistically significant effects in any ERP experiment (and why you shouldn't). *Psychophysiology*. 2017:54:146–157.

Marois A, Labonté K, Parent M, Vachon F. Eyes have ears: indexing the orienting response to sound using pupillometry. *Int J Psychophysiol*. 2018:123:152–162.

Matsuzaki J, Kuschner ES, Blaskey L, Bloy L, Kim M, Ku M, Edgar JC, Embick D, Roberts TPL. Abnormal auditory mismatch fields are associated with communication impairment in both verbal and minimally verbal/nonverbal children who have autism spectrum disorder. *Autism Res*. 2019:12:1225–1235.

Meij B, Venker-van Haagen A, Van den Brom W. Relationship between latency of brainstem auditory-evoked potentials and head size in dogs. *Vet Q*. 1992:14:121–126.

Merzenich MM, Schreiner CE. Mammalian auditory cortex—some comparative observations. In: Popper AN, Webster DB, Fay RR, editors. *Evolutionary biology of hearing*. New York: Springer; 1992. pp. 673–689.

Monteiro P, Feng G. SHANK proteins: roles at the synapse and in autism spectrum disorder. *Nat Rev Neurosci*. 2017:18:147–157.

Murphy PR, O'Connell RG, O'Sullivan M, Robertson IH, Balsters JH. Pupil diameter covaries with BOLD activity in human locus coeruleus. *Hum Brain Mapp*. 2014:35:4140–4154.

Murrell JC, de Groot HN, Venker-van Haagen AJ, van den Brom WE, Hellebrekers LJ. Middle-latency auditory-evoked potential in acepromazine-sedated dogs. *J Vet Intern Med*. 2004:18:196–200.

Naatanen R, Tervaniemi M, Sussman E, Paavilainen P, Winkler I. "Primitive intelligence" in the auditory cortex. *Trends Neurosci*. 2001:24:283–288.

Naatanen R, Paavilainen P, Rinne T, Alho K. The mismatch negativity (MMN) in basic research of central auditory processing: a review. *Clin Neurophysiol*. 2007:118:2544–2590.

Naisbitt S, Kim E, Tu JC, Xiao B, Sala C, Valtschanoff J, Weinberg RJ, Worley PF, Sheng M. Shank, a novel family of postsynaptic density proteins that binds to the NMDA receptor/PSD-95/GKAP complex and cortactin. *Neuron*. 1999:23:569–582.

O'Connor K. Auditory processing in autism spectrum disorder: a review. *Neurosci Biobehav Rev*. 2012:36:836–854.

Petkov CI, Kang X, Alho K, Bertrand O, Yund EW, Woods DL. Attentional modulation of human auditory cortex. *Nat Neurosci*. 2004:7: 658–663.

Phelan K, McDermid HE. The 22q13.3 deletion syndrome (Phelan-McDermid syndrome). *Mol Syndromol*. 2012:2:186–201.

Pincze Z, Lakatos P, Rajkai C, Ulbert I, Karmos G. Effect of deviant probability and interstimulus/interdeviant interval on the auditory N1 and mismatch negativity in the cat auditory cortex. *Brain Res Cogn Brain Res*. 2002:13:249–253.

Ratcliffe VF, Reby D. Orienting asymmetries in dogs' responses to different communicatory components of human speech. *Curr Biol*. 2014:24:2908–2912.

Rendall AR, Perrino PA, Buscarello AN, Fitch RH. Shank3B mutant mice display pitch discrimination enhancements and learning deficits. *Int J Dev Neurosci*. 2019:72:13–21.

Rinne T, Alho K, Ilmoniemi RJ, Virtanen J, Naatanen R. Separate time behaviors of the temporal and frontal mismatch negativity sources. *NeuroImage*. 2000:12:14–19.

Roberts TP, Cannon KM, Tavabi K, Blaskey L, Khan SY, Monroe JF, Qasmieh S, Levy SE, Edgar JC. Auditory magnetic mismatch field latency: a biomarker for language impairment in autism. *Biol Psychiatry*. 2011:70:263–269.

Robertson CE, Baron-Cohen S. Sensory perception in autism. *Nat Rev Neurosci*. 2017:18:671–684.

Sams M, Paavilainen P, Alho K, Naatanen R. Auditory frequency discrimination and event-related potentials. *Electroencephalogr Clin Neurophysiol*. 1985:62:437–448.

Sato Y, Yabe H, Hiruma T, Sutoh T, Shinozaki N, Nashida T, Kaneko S. The effect of deviant stimulus probability on the human mismatch process. *Neuroreport*. 2000:11:3703–3708.

Schreiner CE, Read HL, Sutter ML. Modular organization of frequency integration in primary auditory cortex. *Annu Rev Neurosci*. 2000:23:501–529.

Shiramatsu TI, Takahashi H. Mismatch-negativity (MMN) in animal models: homology of human MMN? *Hear Res*. 2021:399:107936.

Strain GM, Tedford BL, Jackson R. Postnatal development of the brain stem auditory-evoked potential in dogs. *Am J Vet Res*. 1991:52: 410–415.

Tian R, Li Y, Zhao H, Lyu W, Zhao J, Wang X, Lu H, Xu H, Ren W, Tan Q, et al. Modeling *SHANK3*-associated autism spectrum disorder in Beagle dogs via CRISPR/Cas9 gene editing. Under review.

Tremblay MW, Jiang YH. DNA methylation and susceptibility to autism spectrum disorder. *Annu Rev Med*. 2019:70:151–166.

Tu Z, Zhao H, Li B, Yan S, Wang L, Tang Y, Li Z, Bai D, Li C, Lin Y, et al. CRISPR/Cas9-mediated disruption of SHANK3 in monkey leads to drug-treatable autism-like symptoms. *Hum Mol Genet*. 2019:28: 561–571.

Tunturi AR. Physiological determination of the arrangement of the afferent connections to the middle ectosylvian auditory area in the dog. *Am J Physiol*. 1950:162:489–502.

Wang AT, Lee SS, Sigman M, Dapretto M. Neural basis of irony comprehension in children with autism: the role of prosody and context. *Brain*. 2006:129:932–943.

Williams ZJ, Suzman E, Woynaroski TG. Prevalence of decreased sound tolerance (hyperacusis) in individuals with autism spectrum disorder: a meta-analysis. *Ear Hear*. 2021:42: 1137–1150.

Zhao H, Tu Z, Xu H, Yan S, Yan H, Zheng Y, Yang W, Zheng J, Li Z, Tian R, et al. Altered neurogenesis and disrupted expression of synaptic proteins in prefrontal cortex of SHANK3-deficient nonhuman primate. *Cell Res*. 2017:27:1293–1297.

Zhou Y, Kaiser T, Monteiro P, Zhang X, Van der Goes MS, Wang D, Barak B, Zeng M, Li C, Lu C, et al. Mice with Shank3 mutations associated with ASD and schizophrenia display both shared and distinct defects. *Neuron*. 2016:89:147–162.

Zhou Y, Sharma J, Ke Q, Landman R, Yuan J, Chen H, Hayden DS, Fisher JW 3rd, Jiang M, Menegas W, et al. Atypical behaviour and connectivity in SHANK3-mutant macaques. *Nature*. 2019:570: 326–331.